Proceedings of Computational Engineering Conference JSCES
Vol. 28, 2023 May

Wide-area River simulation using 1-m mesh resolution for sediment and flood damage prediction

Arce-Acuna Marlon[1)] 青木 尊之[2)] Shima Hirona[3)] Maya Yoshida[4)]

1) Researcher, Tokyo Institute of Technology (2-12-1 i7-3 Ookayama Meguro, Tokyo, E-mail: marlon.arce@sim.gsic.titech.ac.jp)
2) Professor, Tokyo Institute of Technology (2-12-1 i7-3 Ookayama, Meguro Tokyo, E-mail: taoki@gsic.titech.ac.jp)
3) Researcher, Sabo & Landslide Technical Center
4) Researcher, Sabo & Landslide Technical Center

For a fast, high-resolution river flow, we solve the full shallow water equations using a novel third-order MUSCL numerical scheme accelerated on GPU. Sediment and gravel transportation effects are considered for flood and damage prediction using a benchmark river bed. These simulations were performed completely on GPU and achieved on real time.

Key Words : *Shallow water equations, GPU, River flow, Bed deformation*

1. INTRODUCTION

Flooding are disasters that represent a great risk and damage to cities and their citizens. In recent years, Japan has experienced an increase in river flooding [1], these events make it very important to find ways to forecast flooding.

There are several models that have tried to take on this research. Some one-dimensional models are MIKE11 [2] and HEC-RAS [3], some two-dimensional models include JFLOW [4] and LIS-FLOOD [5]. These represent all good research and efforts to model flooding, it is important to note that in most cases these models use simplifications in the equations or neglect terms in order to obtain fast results.

Since river beds naturally change their shape due to erosion, this effect is important to be studied and included in a model in order to get more accurate results. Some experiments and models [6], [7], have tried this by considering the bed deformation due to sediment particles.

We introduce a model that uses the full shallow water equations to simulate the river flow, with run-up treatment for accurate flooding simulation, as well as presenting the formulation for the river bed deformation.

2. NUMERICAL METHODS

In order to simulate the river flow, we utilize the full shallow water equations (SWE)

$$\frac{\partial \boldsymbol{Q}}{\partial t}+\frac{\partial \boldsymbol{F}}{\partial x}+\frac{\partial \boldsymbol{G}}{\partial y}=S_z+S_\tau+\boldsymbol{R} \qquad (1)$$

$$Q=\begin{bmatrix}h\\M\\N\end{bmatrix}, F=\begin{bmatrix}M\\M^2/h+gh^2/2\\NM/h\end{bmatrix}, G=\begin{bmatrix}N\\MN/h\\N^2/h+gh^2/2\end{bmatrix}, \qquad (2)$$

where h stands for the water height, M and N are the momentum in the x and y direction respectively ($M=hu, N=hv$), z is the river bed, **S** is the source terms (bottom gradient and Manning friction force), **R** is the rainfall source term, g is gravity, and n is the Manning coefficient. The source terms are defined are

$$S_z=\begin{bmatrix}0\\-gh\left(\frac{\partial z}{\partial x}\right)\\-gh\left(\frac{\partial z}{\partial y}\right)\end{bmatrix},$$

$$S_\tau=\begin{bmatrix}0\\\frac{gn^2}{h^{\frac{7}{3}}}\cdot M\sqrt{M^2+N^2}\\\frac{gn^2}{h^{\frac{7}{3}}}\cdot N\sqrt{M^2+N^2}\end{bmatrix},$$

$$\boldsymbol{R}=\begin{bmatrix}R\\0\\0\end{bmatrix}, \qquad (3)$$

where R defines the prescribed rainfall rate [L/s].

These equations are solved using the third-order MUSCL scheme [8] and Local Lax-Friedrichs [9] for element reconstruction. The time integration is based on third-order TVD Runge-Kutta scheme. For the run-up inundation a thin layer technique is used. This method has proved stable, monotone and robust while providing accuracy and speed. For

a detail description of this method with benchmark results and practical applications see [10].

The rainfall term is computed using a Euler time integration, since rainfall data is usually reported in a coarse time and space resolutions, using a first-order integration deemed sufficient.

In order to simulate the river bed deformation due to the sediment, the governing equations [11] are

$$\frac{\partial z_b}{\partial t} + \frac{1}{1-\lambda}\sum_i \left(\frac{\partial q_{bx,i}}{\partial x} + \frac{\partial q_{by,i}}{\partial y}\right) = 0, \tag{4}$$

$$q_{b,i} = \sqrt{sgd_i^3}\left\{17\tau_{*,i}^{3/2}\left(1-\frac{\tau_{*c,i}}{\tau_{*,i}}\right)\left(1-\sqrt{\frac{\tau_{*c,i}}{\tau_{*,i}}}\right)\right\}P_i. \tag{5}$$

Where λ is the porosity of material of bed layer ($\lambda = 0.4$), s is the submerged weight of sediment (chosen as 1.65), $q_{b,i}$ is the sediment transport rate for each size particle i, d_i is the diameter of sediment class for rate for each size particle i. P_i is the fraction in percentage of particle size i in the bed, $\tau_{*,i}$ and $\tau_{*c,i}$ are non-dimensional shear stress of sediment and critical shear stress of sediment respectively. These last two values are computed using the expressions as follows [12],

$$\tau_{*,i} = \frac{u_*^2}{sgd_i}, \tag{6}$$

$$u_* = \sqrt{ghI_e}, \tag{7}$$

$$I_e = \frac{(u^2+v^2)\cdot n^2}{h^{4/3}}. \tag{8}$$

Additionally, it might be necessary to consider the local bed slope (θ) in order to get a more accurate simulation. For this purpose, the following expressions include the slope term (the equations are symmetrical for the y direction)

$$\tau_{*i} = \sqrt{\tau_{*xi}^2 + \tau_{*yi}^2} \tag{9}$$

$$\tau_{*xi} = \frac{u_{*x}\sqrt{u_{*x}^2 + u_{*y}^2}}{sgd_i} + \tau_{*gxi} \tag{10}$$

$$\tau_{*gxi} = \frac{\tau_{*coi}}{\mu_s} sin\theta_x \tag{11}$$

$$sin\theta_x = \frac{z[i-1] - z[i+1]}{\sqrt{(2\Delta x)^2 + \left[z[i-1] - z[i+1]\right]^2}} \tag{12}$$

These equations are solved using an upwind scheme, using the same stability condition for the SWE. Couple and decouple computations between the SWE and bed deformation were tried. Since the numerical results showed no significant difference, we chose to compute the equations separately for computational speed gain.

3. IMPLEMENTATION

1) Domain

In this study, we used two databases to study the river flow with rainfall and the sediment bed deformation.

The first database represents an area of $10{,}500 \times 6{,}000$ meters with a 1-m resolution. This was obtained from a region around the Sumiyoshi river using Lidar technology. The full domain can be seen in Fig. 3. Several of the river routes contain dikes, that have been installed to control the water flow. A second database is provided with the river routes in this area.

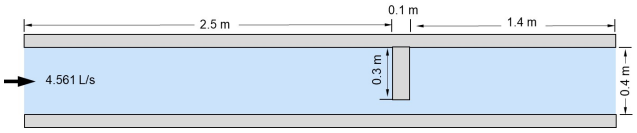

Fig. 1 Bed deformation benchmark description

The second domain describes the bed used to compute the sediment bed deformation [13]. This consist of a bed slope 1:30 of 2 m long and 40 cm wide. There is a block obstacle at 50 cm which is 10 cm wide and 30 cm long. The inflow at the left of the domain is 4.561 L/s, the outflow at the right of the domain is an open boundary.

2) Adaptive block-based computation

Since computing large domains can very computationally demanding, we took the approach to split the domain into blocks and to move to GPU only the blocks that required for active computation. Each block is of size16×16.

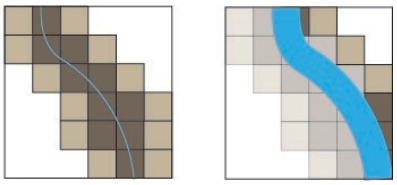

Fig. 2 GPU adaptive block-based computation schematic

All blocks remain on CPU memory. Initially only blocks that contain a river route are uploaded to GPU memory. As the simulation progresses, if the river flow grows or expand and it crosses the boundary of the existing block, then a new neighbor block is upload to GPU memory, this procedure can be seen in Fig. 2. For a more detailed description of this process see [14].

For the Sumiyoshi domain, the total number of blocks is 109,125. However, by using the technique previous described,

only 12,619 blocks are used on GPU memory, and from those 80933 are active blocks. These active blocks represent areas where the simulation is taking place, while the remaining 'inactive' blocks are used for boundary purposes.

3) GPU computation

As previously mentioned, all the computation is performed on GPU. To achieve these, the domain blocks uploaded to GPU memory are computed with a matching CUDA block. Additionally, several optimizations are introduced to compute the different equations and high performance, near peak is obtained.

When needed, in order to speed up the computation of large domains, multi-GPU is used. METIS library [15] is used in these cases to split the domain and obtain load balance for the GPU computation.

4. RESULTS

The first result presented is the river flow with rainfall simulation over the large 1-m resolution Sumiyoshi domain. For this simulation the value R = 0.001 is used.

Since the number of river routes for this area is in the hundreds, a manual initial condition for each route is not feasible. Instead, the domain starts with a dry river bed and the rainfall is used to fill out all the river routes until a steady flow is achieved. Once the steady flow is achieved, this state is stored and used as an initial condition for subsequent simulations.

Fig. 3 shows the Sumiyoshi simulation with the steady flow after running it with rainfall. The zoomed insert in the figure shows the outline of the active blocks as well as it shown the water flow behind a dike located in the river route.

All these computations were performed on GPU, using the University of Tokyo Supercomputer Wisteria-Aquarius, each node with eight A100 Nvidia cards and NVLINK network connection and InfiniBand HDR. Our results were achieved real-time using 2 and 4 GPUs, which makes it possible to use this model for forecasting if necessary.

The second result represents a benchmark to study the bed deformation by sediment. This is very important to incorporate the effect of real bed movement in rivers, particularly with the effect of dikes present in the routes

The initial benchmark has an inflow of 4.651 L/s that moves down a bed with slope 1:30 which contains a block at 50 cm (see Fig. 1). The simulation uses a uniform particle with diameter 0.746 cm. The simulation runs on single GPU real-time due to the size of this domain.

This benchmark is compared to the experimental version described in [13]. Some of the main observations from the experiment are that the water flow creates a "road" behind the mid-block, and that the deepest observed deformation was around 12 cm. Additionally, measurements were performed to present contours of the bed deformation and flow streamlines for the experiment.

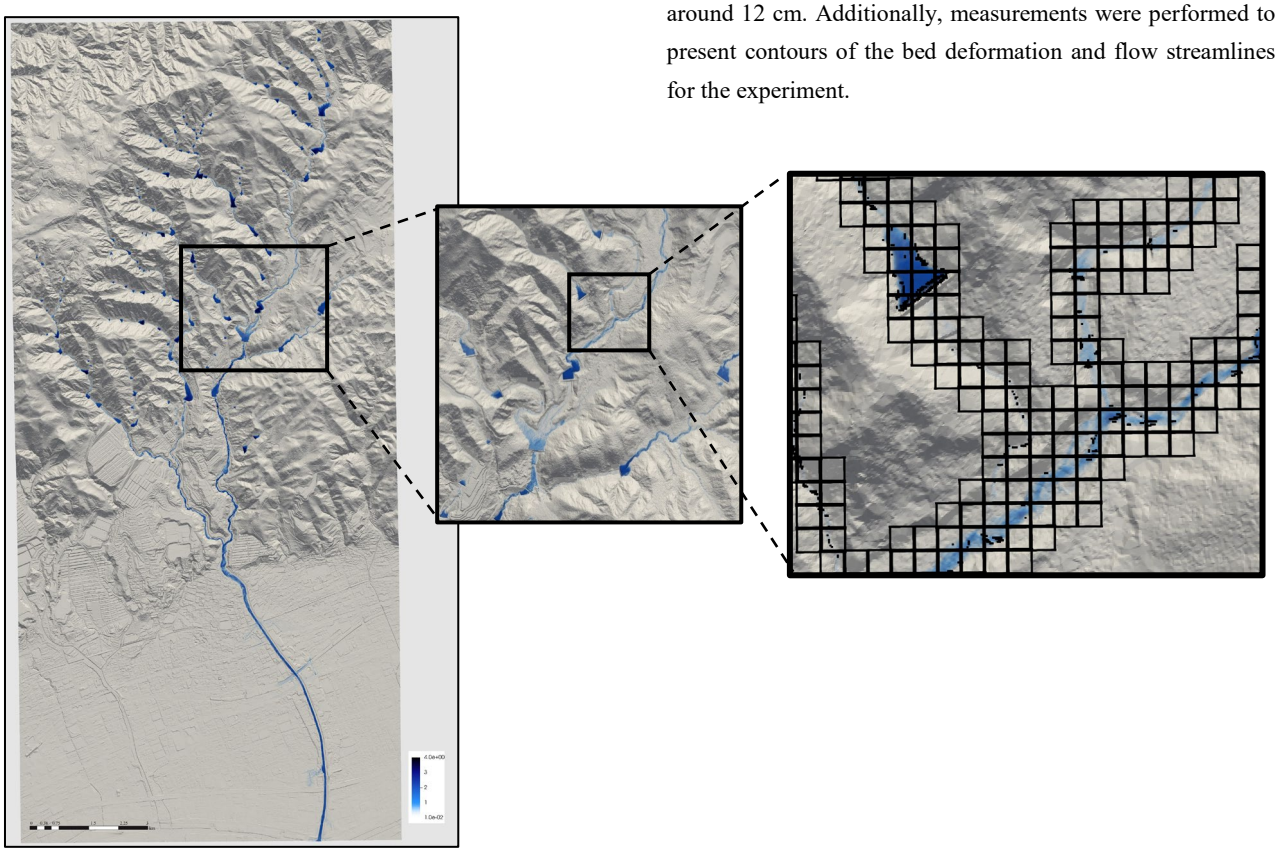

Fig. 3 Sumiyoshi water height of the simulated river flow with steady flow. Insert: sample domain progressive zoom

In our results, we observed a flow 'road' that created behind the mid-block, which is located in good agreement with the location of that reported in the experiment. In the case of the deepest deformation, our simulation obtained around 15.5 cm.

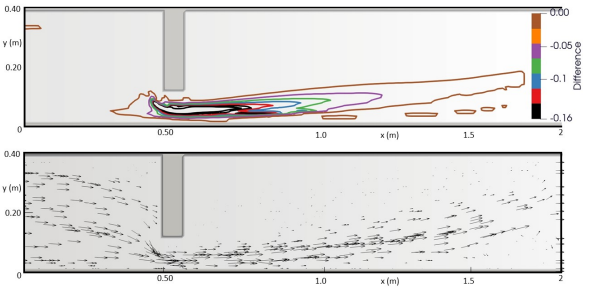

Fig. 4 Bed deformation (Top) and streamlines (Bottom) for sediment benchmark

These differences can be accounted by several factors, such as the numerical method and the boundary conditions used around the bed domain. Results of the flow streamlines and bed deformation contours are shown in Fig. 4 Top and Bottom respectively.

Even though not part of the experiment, in order to further study the effect of sediment on bed deformation, we simulated the same benchmark but using more than a single particle. In total, eight different sizes with their own fraction probabilities were used (see Table 1).

Size (mm)	Percentage (%)
300 >	0
75-300	5.2
19-75	65.8
4.75-19	13.2
2-4.75	5.5
0.85-2	3.1
0.25-0.85	4.5
0.075-0.25	1.9

Table 1 Sediment particle sizes and percentages

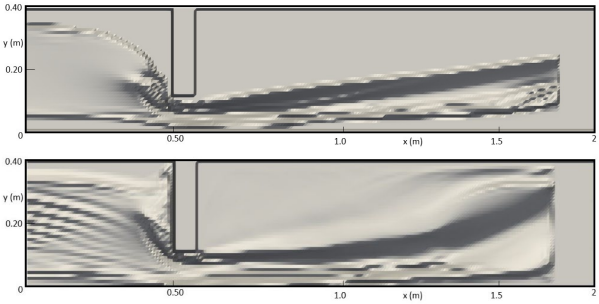

Fig. 5 Bed deformation on benchmark bed using single particle (Top) and multiple particles (Bottom)

The result of this simulation at a steady flow is shown in Fig. 5 bottom, and are compared with the case of a single particle Fig.5 top. As it can be seen, the movement of material of different sizes creates more deformation on the bed than when a single particle is used. Additionally, the deformation with several particles' sizes occurred over a much longer time compared to that of a single particle.

5. CONCLUSIONS

We were able to reproduce the river flow on a real domain using the full SWE. Introducing the rainfall term allowed not only a way to fill out a domain with hundreds of river routes but also to incorporate this value as part of a simulation where rain occurred. The results were obtained fully on GPU in real-time by using four GPUs. The adaptive block-based computation introduced allowed for a fast simulation while preserving the accuracy. The bed deformation simulation was achieved with single and multiple sediment particles and proved that this formulation can be used to simulate the evolution of the deformation on a more realistic and larger domain in the future.

REFERENCES

[1] "The Mainichi Newspaper," 11 August 2022. [Online]. Available: https://mainichi.jp/english/articles/20220811/p2a/00m/0na/005000c. [Accessed 30 September 2022].

[2] H. Danish Hydraulic Institute, MIKE 11 – A Modeling System for Rivers and Channels, 2009.

[3] B. G. W., HEC-RAS River Analysis System: Hydraulic Reference Manual. US Army Corps of Engineers, Institute for Water Resources, Davis, CA.: Hydrologic Engineering Center, 2010.

[4] K. Bradbrook, "JFLOW: a multiscale two-dimensional dynamic flood model," *Water and environment journal,* Vols. https://doi.org/10.1111/j.1747-6593.2005.00011.x, 2006.

[5] J. Shaw, G. Kesserwani, J. Neal, P. Bates and M. K. Sharifian, "LISFLOOD-FP 8.0: the new discontinuous Galerkin shallow-water solver for multi-core CPUs and GPUs," *Geosci. Model Dev,* vol. 14, no. https://doi.org/10.5194/gmd-14-3577-2021, p. 3577–3602, 2021.

[6] S. E. H. T. Xuan Loc Luu, "A new treatment of the exchange layer thickness to evaluate sediment sorting and armoring," *Journal of Applied Mechanics,* vol. 9, pp. 1025-1030, 2006.

[7] H. Z. H. T. C. Z. Luohao Zhang, "Particle size distribution of bed materials in the sandy river bed," *International Journal of Sediment Research,* vol. 32, pp. 331-339, 2017.

[8] S. Yamamoto and H. Daiguji, "Higher-order-accurate upwind schemes for solving the compressible Euler and Navier-Stokes equations," *Comput. Fluids,* vol. 22, pp. 259-270, 1993.

[9] R. J. LeVeque, Finite volume methods for hyperbolic problems, Cambridge, United Kingdom,: Cambridge University Press, 2002.

[10] M. Arce Acuña and T. Aoki, "Tree-based mesh-refinement GPU-accelerated tsunami simulator for real-

time operation," *Nat. Hazards Earth Syst. Sci,* vol. 18, no. https://doi.org/10.5194/nhess-18-2561-2018, pp. 2561-2602, 2018.

[11] M. Hirano, "River-bed degradation with armoring," in *Procs of JSCE*, 1971.

[12] M. Ashida and M. Michiue, "study on hydraulic resistance and bed-load transport rate in alluvial streams," in *Procs of JSCE*, 1972.

[13] N. Kyoichi, M. Masanori and H. Osamu, "Simulation of bed evolution around contration in mountainous river," in *水工学論文集 40th*, 1996.

[14] A.-A. Marlon, A. Takayuki and H. Shima, "A real-time flood simulation with 1m-mesh simulation," in *CMD 35th Computational Mechanics Division Conference*, 2022.

[15] G. Karypis and V. Kumar, "“A Fast and Highly Quality Multilevel Scheme for Partitioning Irregular Graphs”," *SIAM Journal on Scientific Computing,* vol. 20, no. 1, pp. 359-392, 1999.